

## Concomitant polymorphism in the pseudo-peptide Me<sub>2</sub>N-*p*C<sub>6</sub>H<sub>4</sub>C(O)-Phe-OEt

Krunoslav Užarević<sup>a</sup>, Zoran Kokan<sup>b</sup>, Berislav Perić<sup>b</sup>, Nikola Bregović<sup>a</sup>, Srećko I. Kirin<sup>b,\*</sup>

<sup>a</sup> Department of Chemistry, Faculty of Science, University of Zagreb, Horvatovac 102a, HR-10000 Zagreb, Croatia

<sup>b</sup> Ruđer Bošković Institute, Bijenička cesta 54, HR-10000 Zagreb, Croatia

### H I G H L I G H T S

- ▶ Monoclinic (**1m**) and orthorhombic (**1o**) polymorphs of pseudo-peptide **1** were studied.
- ▶ **1m** and **1o** reveal equivalent 2D structures with a different mode of layer stacking.
- ▶ Thermodynamic relations between two polymorphs were unambiguously established.
- ▶ Both polymorphs were prepared in a pure form from solution or by solvent-free methods.
- ▶ Kinetically stable **1m** transfers to thermodynamically stable **1o** by grinding or heating.

### A R T I C L E I N F O

#### Article history:

Received 23 March 2012

Received in revised form 14 July 2012

Accepted 16 July 2012

Available online 25 July 2012

#### Keywords:

Pseudo-peptide

Phenylalanine

Polymorphism

Crystal structure

Solid-state transformations

Mechanochemistry

### A B S T R A C T

Pseudo-peptide Me<sub>2</sub>N-*p*C<sub>6</sub>H<sub>4</sub>C(O)-Phe-OEt (**1**) exhibits two polymorphic forms which crystallizes in non-centrosymmetric space groups, monoclinic **1m** (*P*<sub>21</sub>) and orthorhombic **1o** (*P*<sub>212121</sub>). Both forms occur concomitantly or as a pure phase depending on the solvent of crystallization. Single crystal X-ray diffraction revealed equivalent two-dimensional layers in both **1m** and **1o**, the different modes of layer stacking are caused by C—H···π interactions specific for each polymorph. Both solid forms are transparent in visible spectral region, with different absorbance patterns in lower UV region. Thermodynamic relations between two polymorphs were unambiguously established using room-temperature competitive slurry experiments, mechanochemistry and heating.

© 2012 Elsevier B.V. All rights reserved.

### 1. Introduction

Polymorphism, well known solid-state phenomenon wherein one chemical substance forms two or more crystalline phases [1,2], remains one of the most important topics in modern solid-state chemistry [3,4]. It is mainly manifested through different conformations in flexible molecules and/or different packing arrangements in the crystal structure which molecules assume to achieve free energy minimum. Interest for this phenomenon arises from the fact that polymorphs can display different physicochemical properties, such as crystal habitus, thermal stability, solubility, bioavailability, hygroscopicity, magnetism, color, and electric conductivity. For this reason, polymorphism has developed as a solid state property of paramount importance in materials chemistry [5,6] and pharmaceutical industry, where patenting and material specifications rely on above mentioned properties [7,8].

Compounds that crystallize in non-centrosymmetric groups are widely studied due to their non-linear optical properties and potential applications in laser devices and signal transduction [9,10]. The main prerequisites for applications, such as thermal stability and optical properties, are directly dependable on the orientation of the molecules in the crystal lattice [11]. In some cases, crystallization experiment yields more than one polymorph in the same batch, which is known as concomitant polymorphism [12]. Although such systems result in a batch sample of incoherent physical properties and make control of crystallization process even more demanding, concomitant polymorphs provide valuable data on the thermodynamic and kinetic aspects of the explored system which are inaccessible if only one phase crystallizes.

Recently, we used chiral pseudo-peptides Ph<sub>2</sub>P-*p*C<sub>6</sub>H<sub>4</sub>C(O)-Aa<sub>*n*</sub>-OR, Aa = amino acid, as ligands in Rh(I) catalyzed asymmetric hydrogenation [13]. As an extension of that work, we are interested in the synthesis and structural features of nitrogen analogues Me<sub>2</sub>N-*p*C<sub>6</sub>H<sub>4</sub>C(O)-Aa-OR. In this paper we present solid-state and solution study of two concomitant polymorphs of Me<sub>2</sub>N-*p*C<sub>6</sub>H<sub>4</sub>C(O)-Phe-OEt (**1**), that crystallize in non-centrosymmetric space groups,

\* Corresponding author. Tel.: +385 (0) 1 4561189; fax: +385 (0) 1 4680098.  
E-mail address: [Srecko.Kirin@irb.hr](mailto:Srecko.Kirin@irb.hr) (S.I. Kirin).

monoclinic *P*2<sub>1</sub>, **1m**, and orthorhombic *P*2<sub>1</sub>2<sub>1</sub>2<sub>1</sub>, **1o**. The analysis of common and distinct intermolecular interactions was based on X-ray single crystal structures. Solution properties were investigated by NMR and UV–Vis spectrometry, while solid-state UV–Vis measurements were employed to determine the absorbance cut-off of crystalline phases. Competitive slurry experiments [14,15] were combined with solvent-free methods (grinding and heating) [16] to precisely establish relative thermodynamic relations between two polymorphs.

## 2. Experimental section

### 2.1. General remarks

Synthesis was carried out in ordinary glassware; chemicals were used without further purification. Nuclear magnetic resonance spectra (NMR) were collected with a Bruker Avance 300 MHz spectrometer. Chemical shifts,  $\delta$ /ppm, indicate a downfield shift from tetramethylsilane, TMS, the internal standard. Coupling constants, *J*, are given in Hz. Individual peaks are marked as: singlet (s), doublet (d), triplet (t), quartet (q) or multiplet (m). UV–Vis measurements were carried out on Varian Cary 5 double beam spectrophotometer equipped with a thermostat device. Infrared spectra (IR) were recorded on a PerkinElmer Spectrum RXI FT-IR spectrometer from dried samples dispersed in KBr pellets (4000–400 cm<sup>-1</sup> range, step 2 cm<sup>-1</sup>). Positive ion electrospray mass spectra (ES + MS) were measured on an Agilent 6410 Triple Quadrupole Mass Spectrometer. Powder X-ray diffraction (PXRD) experiments were performed on a Philips PW 3710 diffractometer, Cu K $\alpha$  radiation, flat plate sample on a zero background in Bragg–Brentano geometry, voltage 40 kV, and current 40 mA. The patterns were collected in the angle region between 4° and 40° (2 $\theta$ ) with a step size of 0.02° and 1.0 s counting per step. Single-crystal X-ray diffraction (SCXRD) was performed on an Oxford Diffraction Xcalibur CCD diffractometer with graphite-monochromated Mo K $\alpha$  radiation in a nitrogen vapor stream at 120 K using  $\omega$ -scans. Mechanochemical routine: samples were neat ground in steel jars using

Retsch MM200 ball mill (25 Hz) for 30 min. After such treatment PXRD patterns were collected. Differential scanning calorimetry (DSC) was performed on the Mettler–Toledo DSC823<sup>e</sup> calorimeter with STARe SW 9.01 in the range from 25 to maximally 250 °C (5 °C min<sup>-1</sup>) under the nitrogen stream. Thermogravimetric analysis (TGA) was performed on a Mettler–Toledo TGA/SDTA851<sup>e</sup> thermobalance using alumina crucibles under nitrogen stream with the heating rate of 5 °C min<sup>-1</sup>. In all experiments the temperature ranged from 25 to 250 °C. The results were processed with the Mettler STARe 9.01 software.

### 2.2. Synthesis

4-Dimethylaminobenzoic acid (412 mg, 2.5 mmol), TBTU (800 mg, 2.5 mmol) and HOBt (339 mg, 2.5 mmol) were dissolved in acetonitrile (100 ml, p.a.) in a 250 mL round bottomed flask at room temperature. DIPEA (1.7 mL, 10 mmol) was added and the clear greenish solution was continued stirring for 1 h. Then L-phenylalanine ethyl ester (574 mg, 2.5 mmol) was added and the stirring was continued overnight. Acetonitrile was evaporated *in vacuo* and ethyl-acetate (100 ml) was added to the oily residue, washed with NaHCO<sub>3</sub> (100 mL, sat. aq.) and H<sub>2</sub>O (2 × 100 mL), dried over anhydrous Na<sub>2</sub>SO<sub>4</sub>, filtered and evaporated to dryness to give a pale green solid residue. The residue was purified by column chromatography (silica, 50 g, Et<sub>2</sub>O/MeOH (100:1), TLC: *R*<sub>f</sub> = 0.36) and eluted with diethyl ether (50 mL) and then with Et<sub>2</sub>O/MeOH (100:1). Peak fractions were evaporated to dryness to give 624 mg (77%) of white crystalline product. <sup>1</sup>H NMR (300 MHz, CDCl<sub>3</sub>)  $\delta$ /ppm: 1.26 (t, 3H, *J* = 7 Hz, H<sub>Et</sub>), 3.02 (s, 6H, H<sub>NMe</sub>), 3.18–3.30 (m, 2H, H $\beta$ ), 4.19 (q, 2H, *J* = 7 Hz, H<sub>Et</sub>), 5.06 (dt, 1H, *J*<sub>1</sub> = 7.5 Hz, *J*<sub>2</sub> = 5.5 Hz, H $\alpha$ ), 6.44 (d, 1H, *J* = 7.5 Hz, H<sub>NH</sub>), 6.63–6.68 (m, 2H, H<sub>Ph-2,6</sub>), 7.13–7.31 (m, 5H, H<sub>Bz</sub>), 7.62–7.67 (m, 2H, H<sub>Ph-3,5</sub>); <sup>13</sup>C NMR (300 MHz, CDCl<sub>3</sub>)  $\delta$ /ppm: 14.27 (C<sub>Et</sub>), 38.29 (C $\beta$ ), 40.21 (C<sub>NMe</sub>), 53.51 (C $\alpha$ ), 61.55 (C<sub>Et</sub>), 120.67 (C<sub>Ph-1</sub>), 111.15 (C<sub>Ph-3,5</sub>), 126.99 (C<sub>Bz-p</sub>), 128.46, 128.55 (C<sub>Bz-o,m</sub>), 129.49 (C<sub>Ph-2,6</sub>), 136.34 (C<sub>Bz-i</sub>), 152.74 (C<sub>Ph-4</sub>), 166.78 (CO<sub>amide</sub>), 172.08 (CO<sub>ester</sub>); IR (KBr)  $\nu$ /cm<sup>-1</sup>: **1m**: 3371 (sharp,  $\nu_{N-H}$ ); 1747 (sharp,  $\nu_{C=O}$ ); 1634, 1608, 1504 (all  $\nu_s$ , mixed C=O, C=C); **1o**: 3370 (sharp,  $\nu_{N-H}$ ); 1750 (sharp,  $\nu_{C=O}$ ); 1631, 1610, 1507 (all  $\nu_s$ , mixed C=O, C=C); MS (ES+), *m/z*: 148.1 ([M–Phe]<sup>+</sup>, 100%), 341.2 ([M + H]<sup>+</sup>, 33.2 ([M + Na]<sup>+</sup>). Single crystals suitable for X-ray diffraction were obtained by slow evaporation of solvent mixtures Et<sub>2</sub>O/MeOH (100:1) for **1m** and EtOAc/hexane (4:1) for **1o**.

### 2.3. Crystallization experiments

For each crystallization experiment, 5 mg of the sample was dissolved in 1 mL of an assorted solvent in a test tube and the solutions were left for slow evaporation at room temperature. Solvents (methanol, ethanol, n-propanol, acetone, acetonitrile, chloroform, dichloromethane and diethyl ether) were selected by their protic and dielectric properties. Pseudo-peptide **1** proved insoluble in diethyl ether. In alcohols, **1** would crystallize after 20 h standing and the samples were filtrated and dried at air. From other solvents, no crystallization occurred until the solvent completely evaporated. In the second set of experiments, 3 mL of diethyl ether was added to the respective solutions, which was followed by almost immediate precipitation of the product. PXRD spectra were collected for all obtained samples.

### 2.4. X-ray single-crystal diffraction

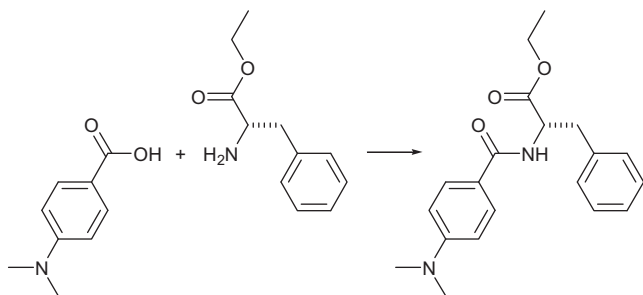
Details of data collection and crystal structure refinement are given in Table 1. Program CrysAlisPro [17] was used for data collection, cell refinement, and data reduction. Sample **1m** was twinned, consisting of two components where one was more dominant. The

**Table 1**  
Crystallographic data for **1m** (monoclinic) and **1o** (orthorhombic) polymorphs.

	<b>1m</b>	<b>1o</b>
Empirical formula	C <sub>20</sub> H <sub>24</sub> N <sub>2</sub> O <sub>3</sub>	C <sub>20</sub> H <sub>24</sub> N <sub>2</sub> O <sub>3</sub>
Formula weight (g mol <sup>-1</sup> )	340.41	340.41
Crystal system	Monoclinic	Orthorhombic
Crystal size (mm <sup>3</sup> )	0.03 × 0.03 × 0.5	0.07 × 0.1 × 0.3
Crystal habitus	Needle	Prism
Crystal color	Colorless	Colorless
Space group	<i>P</i> 2 <sub>1</sub>	<i>P</i> 2 <sub>1</sub> 2 <sub>1</sub> 2 <sub>1</sub>
Unit cell dimensions (Å, °)		
<i>a</i>	11.2142(6)	5.3521(2)
<i>b</i>	5.4222(3)	14.5692(4)
<i>c</i>	14.597(1)	22.9904(7)
$\alpha$	90.00	90.00
$\beta$	94.440(5)	90.00
$\gamma$	90.00	90.00
Volume (Å <sup>3</sup> )	884.92(9)	1792.70(10)
<i>Z</i>	2	4
<i>D</i> <sub>calc</sub> (g cm <sup>-3</sup> )	1.278	1.261
$\mu$ (mm <sup>-1</sup> )	0.086	0.085
<i>F</i> (000)	364	728
Reflections collected/unique	8089/4802	24242/4162
Data/restraints/parameters	4802/1/233	4162/0/233
Goodness-of-fit on <i>F</i> <sup>2</sup> , <i>S</i> <sup>a</sup>	0.922	1.068
<i>R</i> / <i>wR</i> [ <i>I</i> > 2 $\sigma$ ( <i>I</i> )] <sup>b</sup>	0.0652/0.1029	0.0332/0.0816
Largest diff. peak/hole (eÅ <sup>-3</sup> )	0.257/–0.240	0.172/–0.140

<sup>a</sup>  $S = \sum [w(F_o^2 - F_c^2)^2] / (N_{obs} - N_{param})^{1/2}$ .

<sup>b</sup>  $R = \sum |F_o| - |F_c| / \sum |F_o|$ ;  $wR = [\sum w(F_o^2 - F_c^2)^2 / \sum (F_o^2)^2]^{1/2}$ ,  $w = 1 / [\sigma^2(F_o^2) + (g_1 P)^2 + g_2 P]$  where  $P = (F_o^2 + 2F_c^2) / 3$ .



**Scheme 1.** Reaction conditions: (a) TBTU/HOBT/DIPEA, CH<sub>3</sub>CN, R.T., 16 h, 77%.

observed intensities (“hkl file”) for this sample were produced by extraction of reflections only from the more dominant component. The structures were solved by direct methods using SIR97 program [18]. The full-matrix least-squares refinements based on  $F^2$  against all reflections were performed using SHELXL97 program [19]. The refinements included anisotropic displacement parameters for all non-H atoms and isotropic displacement parameters for all hydrogen atoms. The hydrogen atoms, except H(9) (involved in the hydrogen bond), were positioned geometrically and refined in the riding model [ $C-H = 0.93-0.98 \text{ \AA}$ ;  $U_{iso}(H) = 1.2 \text{ or } 1.5 \times U_{eq}(C)$ ]. Torsion angles of methyl groups around the bonds they form with other non-H atoms were refined. Position of H(9) atom in both polymorphs was determined from the difference Fourier maps, it was included in the refinements unconstrained and with unrestrained isotropic thermal parameter. Calculations were performed using programs within WinGX program package [20]. Geometry calculations were done by PLATON program [21] and the molecular graphics were done by PLATON, ORTEPIII [22] and Mercury [23] programs.

### 2.5. UV–Vis spectrophotometric measurements

The solution spectra of **1** ( $c \approx 3.5 \times 10^{-5} \text{ mol dm}^{-3}$ ) were recorded in methanol and chloroform (600–240 nm), using quartz cells with 1 cm optical path. In order to obtain solid-state spectra of both polymorphs, pellets with  $\approx 0.1 \text{ mg}$  of sample (**1m** or **1o**) dispersed in KBr ( $m \approx 50 \text{ mg}$ ) were recorded against pellets of pure KBr used as reference sample. To investigate the influence of high temperature on the solid state UV–Vis spectrum of **1m**, the sample pellet was heated to  $125 \text{ }^\circ\text{C}$  ( $3 \text{ }^\circ\text{C min}^{-1}$ ) in the laboratory oven, held at that temperature for 45 min, and the spectrum was recorded after cooling.

### 2.6. Competitive slurry experiments

15 mg of the sample mixture containing **1m** (7 mg) and **1o** (8 mg) was added to n-propanol/diethyl ether solvent system (2 mL, 1:1). Resulting slurry was stirred for 5 h at the room temperature. Solid sample was immediately filtrated and analyzed by PXRD.

## 3. Results and discussion

### 3.1. Synthesis and identification

The title compound Me<sub>2</sub>N-*p*-C<sub>6</sub>H<sub>4</sub>(O)-Phe-OEt (**1**) was synthesized by standard peptide coupling in solution using the TBTU/HOBT/DIPEA protocol and obtained in good yield (77%) after purification by column chromatography on silica, Scheme 1. Pseudo-peptide **1** was characterized by <sup>1</sup>H, <sup>13</sup>C NMR and IR spectroscopy and positive-ion electrospray mass spectrometry, ES + MS.

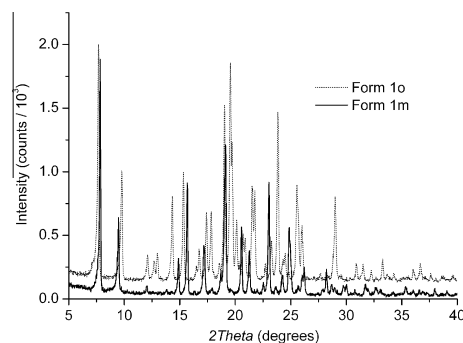


**Fig. 1.** Room temperature PXRD spectra for **1m** and **1o** forms.

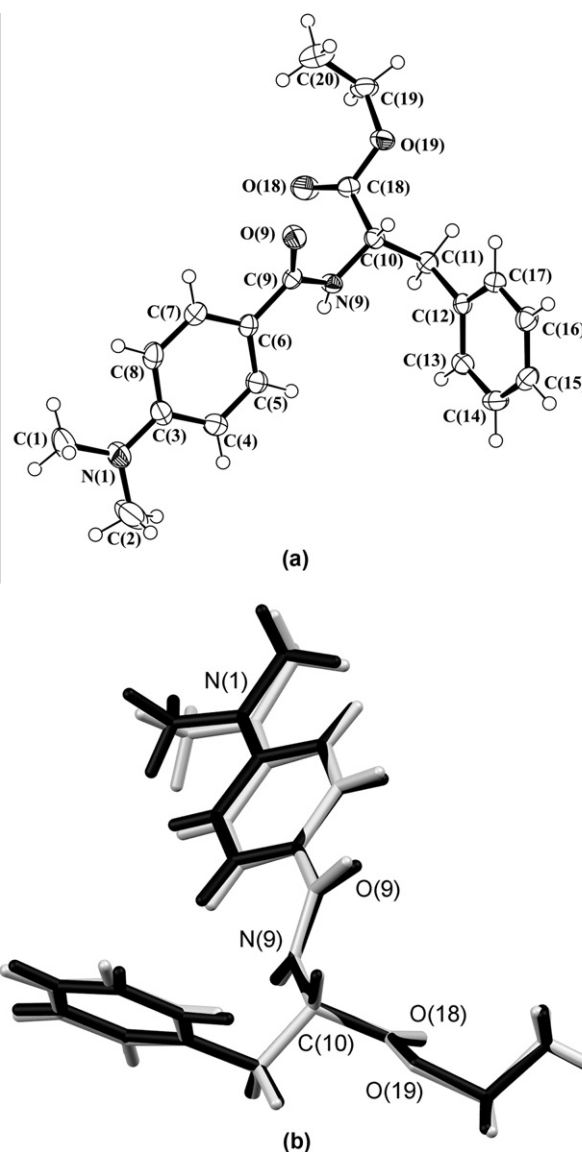


**Fig. 2.** (a) ORTEPIII [22] view of molecule of the title compound in **1o** form. Ellipsoids are drawn at the 50% probability level. Hydrogen atoms are presented as spheres of arbitrary small radii. (b) Overlapped molecular structures of **1m** (colored), and **1o** (violet).

### 3.2. Crystallization experiments

Compound **1** was crystallized from different solvent mixtures in order to prepare single crystals suitable for crystallographic

analysis. Two polymorphs of **1** were obtained depending on the solvent of crystallization. Slow evaporation of an Et<sub>2</sub>O/MeOH (100:1) solution of **1** at room temperature yielded single crystals of monoclinic polymorph **1m** (colorless needles), while colorless prism of orthorhombic polymorph **1o** were obtained from EtOAc/hexane (4:1) solution. Experimental PXRD spectra, Fig. 1, compared to those calculated from single-crystals and refined in TOPAS [24], showed that bulk samples from both solutions were mixtures of **1m** (dominant) and **1o** phases (see Supplementary Material). Screening crystallization experiments revealed the following: concomitant mixture of **1m** and **1o** crystals (dominant) was obtained from alcohols (methanol, ethanol, n-propanol), while the crystallization from dichloromethane yielded concomitant mixture of **1m** (dominant) and **1o**. In all cases, addition of diethyl ether as precipitant [25] to a solution resulted in pure **1m** microcrystalline product. Pure **1m** was also obtained from acetone or chloroform, while crystallization from acetonitrile yielded pure **1o** phase.

#### 4. Single crystal structure

Single crystal structures were determined for both **1m** (needles, monoclinic, *P2*<sub>1</sub>) and **1o** (prisms, orthorhombic, *P2*<sub>1</sub>*2*<sub>1</sub>*2*<sub>1</sub>); the structure of **1o** together with the atom numbering scheme is depicted in Fig. 2a. Molecular structures of both **1m** and **1o** have identical conformation, the comparison of the molecular structures in **1m** and **1o** forms is presented in Fig. 2b, the differences in analogous bond lengths are less than their 4 standard deviations and analogous bond or torsion angles differ for less than 1° or 5°, respectively. Several common features are found in molecular structures of both polymorph forms:

- (i) The (CH<sub>3</sub>)<sub>2</sub>N-group contains *sp*<sup>2</sup> hybridized N(1) atom and is planar. The (CH<sub>3</sub>)<sub>2</sub>N-group is twisted with respect to the central phenyl Ph(1) ring with dihedral angle between the respective planes equal to 12.7(3)° and 9.24(17)° in **1m** and **1o** form, respectively.
- (ii) Twisting of amide plane defined by atoms C(9), O(9) and N(9) with respect to the central phenyl ring Ph(1) is identical in both polymorphs, 25.5(3)° and 25.64(13)° for **1m** or **1o** forms, respectively.

- (iii) Torsion angle C(9)—N(9)—C(10)—C(18) ( $\varphi$  angle in peptides) [26], having values of  $-83.7(3)^\circ$  and  $-79.89(13)^\circ$  in **1m** or **1o** forms, respectively, is not representative for any secondary peptide structure (e.g. for  $\alpha$ -helix or  $\beta$ -sheet). The angle N(9)—C(10)—C(11)—C(12) ( $\chi$  angle in peptides) [26] with value of  $-65.5(2)^\circ$  and  $-69.75(12)^\circ$  in **1m** and **1o** forms, respectively, indicate gauche<sup>-</sup> conformation of the phenylalanine side chain.
- (iv) The torsion angle N(9)—C(10)—C(18)—O(18) exhibit a *cis* conformation of the ester's C(18)—O(18) carbonyl group with value of  $-16.7(3)^\circ$  or  $-19.39(16)^\circ$  in **1m** or **1o** form, respectively.

Intermolecular interactions in **1m** and **1o** polymorph forms are listed in Table 2. The most important intermolecular interaction is the hydrogen bond formed between two amide groups from neighboring molecules and is common for both polymorphs, Fig. 3a. In addition, structure of both polymorphic forms is stabilized by C—H... $\pi$  interactions, Fig. 3b. First, a contact of the C(14)—H(14) group from Ph(2) ring from one molecule (A in Fig. 3b) with the  $\pi$  system of the Ph(2)<sup>ii</sup> ring from the neighboring molecule (A<sup>ii</sup> in Fig. 3b) is found. And second, the contact between the C(8)—H(8) group of Ph(1) ring from one molecule (A in Fig. 3b) and  $\pi$  system of Ph(1)<sup>iii</sup> ring from another neighboring molecule (A<sup>iii</sup> in Fig. 2b) can be considered as a weak C—H... $\pi$  interaction, Table 2.

The three common intermolecular contacts described above, one hydrogen bond and two C—H... $\pi$  interactions, are responsible for the aggregation of molecules in two-dimensional layers equivalent for both **1m** and **1o** forms, Table 2 and Fig. 3b. Basic repetition motif in these layers lies in the *b*<sub>m</sub>*c*<sub>m</sub> plane of monoclinic unit cell, or in the *a*<sub>o</sub>*b*<sub>o</sub> plane of orthorhombic unit cell.

Intermolecular interactions specific to each polymorph form are C—H... $\pi$  interactions with an aliphatic donor C—H group. In particular, a C(19)—H(19B)...Ph(2)<sup>iv</sup> contact was found in **1m**, while a C(20)—H(20B)...Ph(2)<sup>iv</sup> interaction is present in **1o**, Table 2. These distinct intermolecular interactions are clearly visible in the Hirshfeld surface fingerprint plots [27,28], Fig. 4. They are responsible for the different packing of the identical two-dimensional layers in the crystals of **1m** and **1o**. In **1m** the layers are simply stacked (translated) in a parallel fashion one above the other along direction of the monoclinic unit cell axis *a*<sub>m</sub>, Fig. 5a, while in **1o** the

**Table 2**  
Intermolecular interactions in **1m** and **1o** forms.

Interactions common for both polymorphs (Fig. 3):					
Hydrogen bonds					
Form	D—H...A	D—H (Å)	H...A (Å)	D...A (Å)	D—H...A (°)
<b>1m</b>	N(9)—H(9)...O(9) <sup>ia</sup>	0.84(3)	2.44(3)	3.265(3)	166(2)
<b>1o</b>	N(9)—H(9)...O(9) <sup>ib</sup>	0.852(16)	2.380(16)	3.2072(14)	163.9(13)
C—H... $\pi$ interactions					
Form	C—H... $\pi$	C—H (Å)	H... $\pi$ (Å)	C... $\pi$ (Å)	C—H... $\pi$ (°)
<b>1m</b>	C(14)—H(14)...Ph(2) <sup>ii,a</sup>	0.93	2.90	3.636(2)	137
<b>1o</b>	C(14)—H(14)...Ph(2) <sup>ii,b</sup>	0.93	2.94	3.6923(15)	138
<b>1m</b>	C(8)—H(8)...Ph(1) <sup>iii,a</sup>	0.93	3.06	3.715(3)	128
<b>1o</b>	C(8)—H(8)...Ph(1) <sup>iii,b</sup>	0.93	3.10	3.7157(15)	125
Interactions specific for each polymorph (Fig. 5):					
C—H... $\pi$ interactions					
Form	C—H... $\pi$	C—H (Å)	H... $\pi$ (Å)	C... $\pi$ (Å)	C—H... $\pi$ (°)
<b>1m</b>	C(19)—H(19B)...Ph(2) <sup>iv,a</sup>	0.97	2.54	3.425(3)	151
<b>1o</b>	C(20)—H(20B)...Ph(2) <sup>iv,b</sup>	0.96	2.87	3.6290(18)	137

<sup>a</sup> Symmetry codes: (i) *x*,  $-1 + y$ , *z*; (ii)  $-x$ ,  $-1/2 + y$ ,  $1 - z$ ; (iii)  $-x$ ,  $1/2 + y$ ,  $-z$ ; and (iv)  $1 - x$ ,  $1/2 + y$ ,  $1 - z$ .

<sup>b</sup> Symmetry codes: (i)  $-1 + x$ , *y*, *z*; (ii)  $-1/2 + x$ ,  $3/2 - y$ ,  $-z$ ; (iii)  $1/2 + x$ ,  $1/2 - y$ ,  $-z$ ; and (iv)  $1 - x$ ,  $-1/2 + y$ ,  $1/2 - z$ .

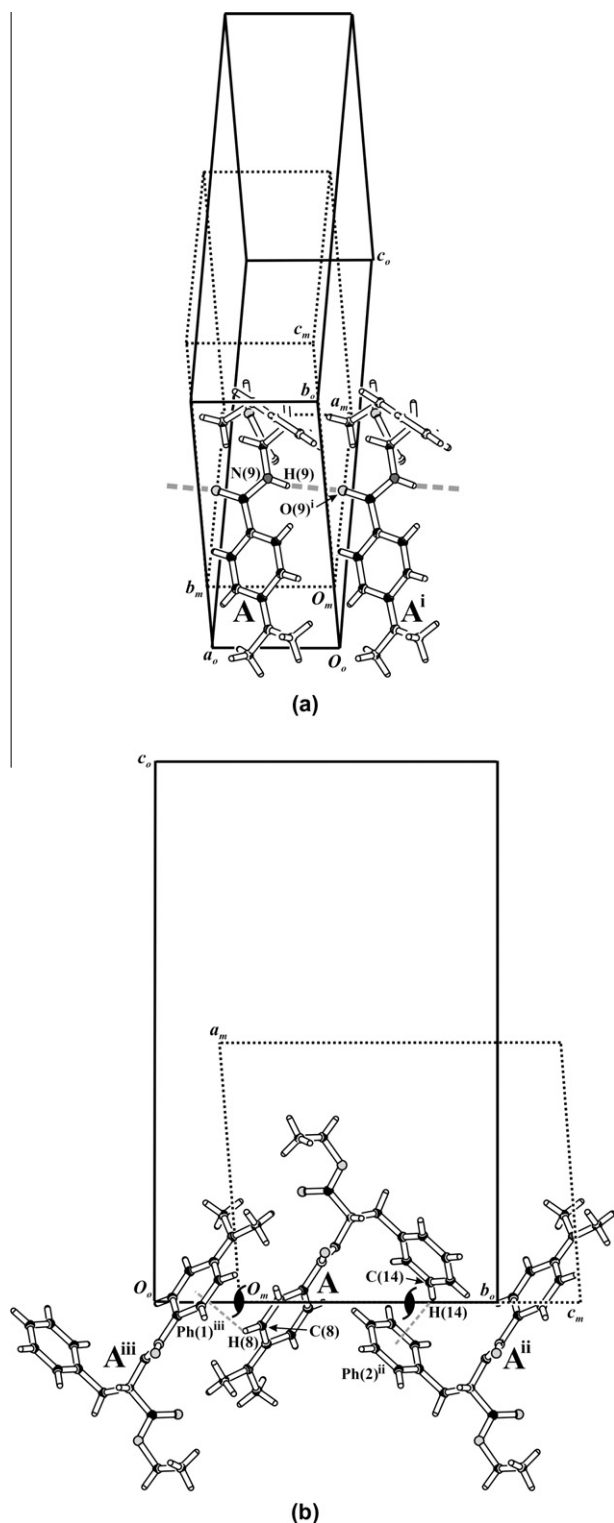


**Fig. 3.** Common intermolecular interactions responsible for formation of two-dimensional isostructural layers in both polymorphs: (a) Hydrogen bond N(9)–H(9)···O(9)<sup>i</sup>, (b) C–H··· $\pi$  interactions [C(14)–H(14)···Ph(2)<sup>ii</sup> and C(8)–H(8)···Ph(1)<sup>iii</sup>]. Symmetry codes are given in Table 2. Unit cells for orthorhombic and monoclinic forms are shown by full and dotted black lines, respectively. Interactions are denoted by gray dashed lines. View on (b) is along  $b_m$  axis of **1m** form or along  $a_o$  axis of **1o** form.

layers are stacked in an antiparallel fashion (rotated for 180°) one above the other around  $c_o$ , the axis perpendicular to the layers, Fig. 5b.

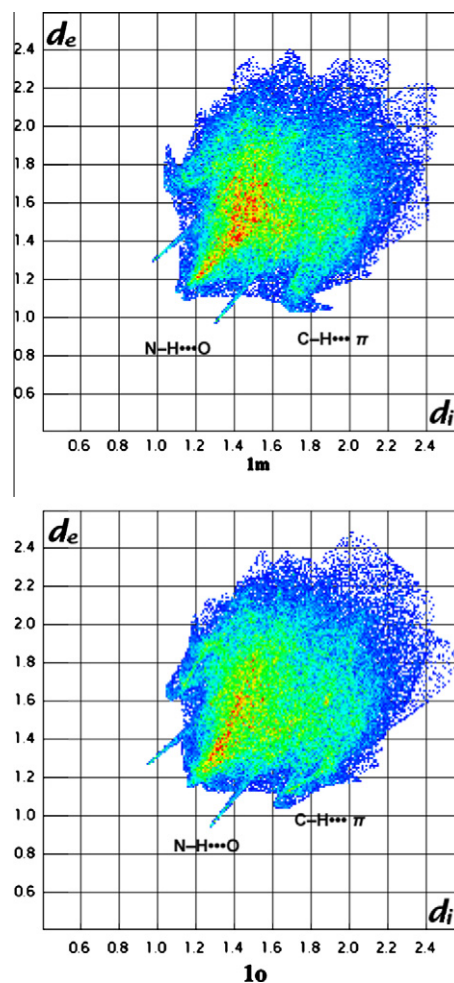


**Fig. 4.** Hirshfeld surfaces fingerprint plots for polymorph forms **1m** and **1o**. While the N–H···O interactions are similar in both forms (presented by sharp spikes), the C–H··· $\pi$  intermolecular contacts are more pronounced in the structure of **1m** (side-wings). (For interpretation to colours in this figure, the reader is referred to the web version of this paper.)

Exploring only organic compounds from Cambridge Structural database (CSD) [29], a number of biologically interesting compounds including carcinogenic toxin Aflatoxin [30], antidiabetic drug Chlorpropamide [31,32], and naturally occurring plant quinine  $\beta$ -lapachone [33] revealed a layer polymorphism with features similar to **1m/1o**: (a) the two polymorphs differ only in the relative stacking of identical two-dimensional layers, (b) the two polymorphs crystallize in monoclinic  $P2_1$  and orthorhombic  $P2_12_12_1$  groups, respectively (although in some literature cases additional polymorphs are known as well), and (c) in both polymorphs two axis are of equal length, while the third axis is twice as long in the orthorhombic polymorph.

## 5. Spectrophotometric investigations

Since the crystallization product varied depending on the used solvent, UV–Vis spectra of **1** in protic and aprotic solvents of different polarities were recorded to gain more insight into the solvent effect, Fig. 6a. Slight increase in absorbance of the band at 306 nm was observed for methanol solution. The corresponding band can be assigned to the excitation of the benzene rings. The similarity of the obtained UV–Vis spectra indicates that there is no significant impact of the solvent proticity on the specific solvent-pseudo-peptide **1** interactions [34]. No direct correlation

between the solution behavior and crystallization outcomes can be established.

Transparency of the material in visible spectral region is one of the prerequisites for their potential optical application. Solid state UV spectra of both polymorphs showed similar characteristics; both **1m** and **1o** being transparent in the visible spectral region, from 800 to 370 nm, Fig. 6b. In the UV spectral range two absorption bands appeared. One band was positioned at 210 nm for both forms, while the other occurred at 290 nm for **1m** or at 285 nm in the spectrum of **1o**. It should also be noted that a significant correlation between spectra in the solid state and solution was observed, with slight hypsochromic shift of the characteristic maximum in solution. Since the absorption cut-off wavelength of **1** is in UV region, both polymorphs would be adequate for optical studies. Although both polymorphs are non-centrosymmetric and thus sustainable for the second order non-linear optical (NLO) behavior [35], different modes of layers staking could induce larger differences in NLO characteristics [36] than in spectrophotometric properties presented here.

## 6. Thermal and mechanochemical reactivity

The relative thermodynamic relations of two polymorph forms **1m** and **1o** and the possibility of their thermally or mechanochemically induced solid-state interconversions were investigated by means of differential scanning calorimetry (DSC), thermogravimetric analysis (TGA) and neat grinding. DSC measurements of form **1m** in nitrogen atmosphere revealed a weak endothermic peak at 110 °C followed by strong endothermic peak at 137 °C (onset), Fig. 7. To establish whether the first thermal event corresponds to a transformation of **1m** to a new phase, **1m** was heated to 120 °C and allowed to cool to room temperature. PXRD identified this sample as pure **1o**, i.e. the endotherm at 110 °C corresponds to a phase change of **1m** → **1o**. Consequently, the strong endotherm at 137 °C corresponds to melting of pure **1o**; melting point of **1m** was thus not possible to determine. No mass loss was observed during both thermal events (TGA). Thermally induced **1m** → **1o** phase transition is irreversible. When **1m** or **1o** samples were heated to 145 °C and the melt cooled to room temperature,

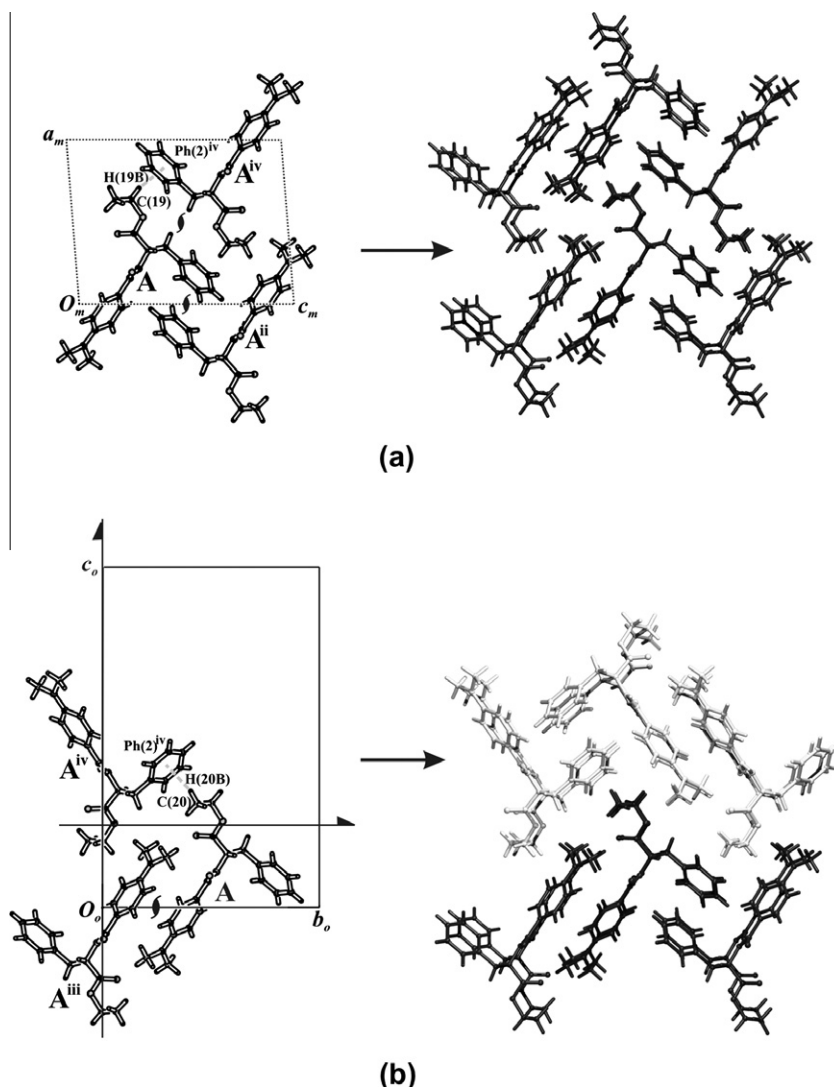


**Fig. 5.** Distinct intermolecular interactions: (a) C(19)—H(19B)···Ph(2)<sup>iv</sup> specific for **1m** form and (b) C(20)—H(20B)···Ph(2)<sup>iv</sup> specific for **1o** form. Symmetry codes are given in Table 2. Interactions are denoted as gray dashed lines on the left part of the figures. Twofold symmetry axes characteristic for these interactions are also shown. Right parts of the figures are perspective views of crystal structures where opposite orientations of successive layers are denoted in black and white color for **1o** form (b). In **1m** form all layers have the same orientation (black). Views are same as in Fig. 3b.

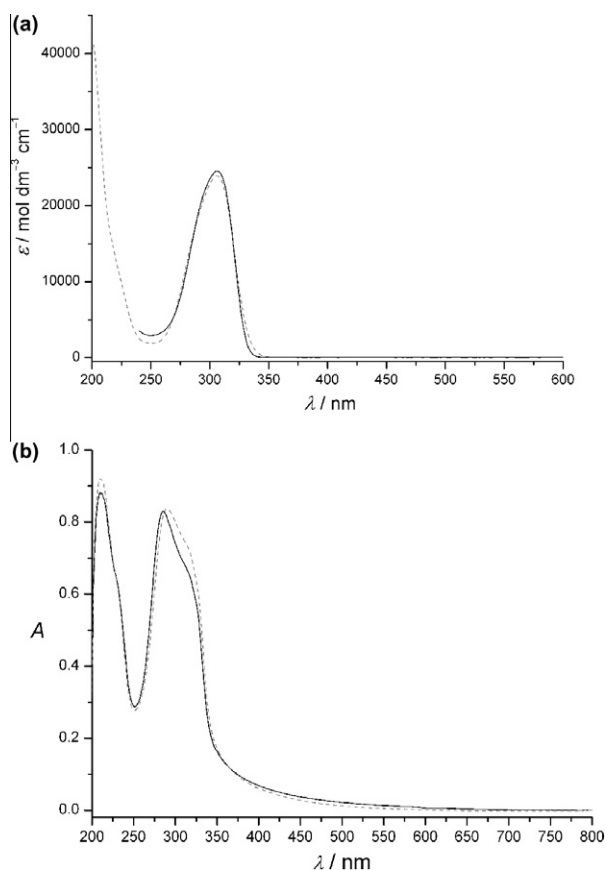


**Fig. 6.** (a) Electronic absorption spectra of **1** in chloroform (—) and methanol (---) at 25 °C. (b) Solid-state UV-Vis spectra of **1o** (—) and **1m** (---) polymorphs in KBr pellet ( $w = 2\%$ ) at 25 °C.

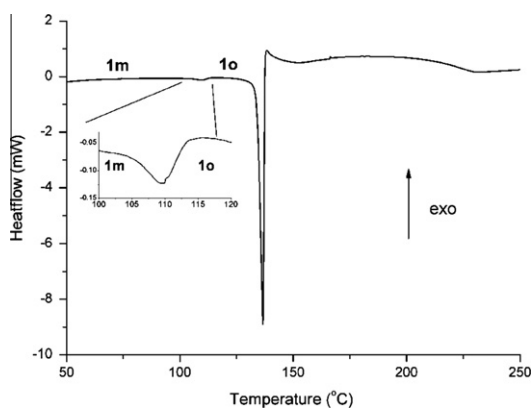


**Fig. 7.** DSC trace of **1m** form. The inset represents the thermal event corresponding to the transformation of **1m** to **1o**. The sharp endothermic peak corresponds to melting of **1o** form.

the resulting solid was pure **1m**, independent of the cooling rate (30 or 1 °C min<sup>-1</sup>) (see ESI).

Mechanochemical methods have recently proved as a viable alternative for the synthesis of new materials which were hardly obtainable from solution [37,38], and also for the resolution of polymorphs in various systems [39–41]. Neat grinding (25 Hz, 30 min, room temperature) in a ball mill induced irreversible **1m** → **1o** transformation, while **1o** was stable during grinding. Re-

sults imply that same polymorph, **1o**, is thermodynamically stable both at high temperature (DSC) and at low temperature (grinding). However, there were some examples reported where the grinding yielded metastable polymorph [42]. Also, one should not exclude possibility that, during the grinding process, localized parts of sample would be heated by friction and by impact with the ball inside the jar [16,43]. Therefore, further experiments needed to be employed to unambiguously determine thermodynamic relation in this system.

## 7. Relative thermodynamic stability

In this system, we were not able to determine melting points for both polymorphs, due to **1m** → **1o** solid phase transition and consequently, the “heat of fusion” rule to distinguish between a monotropic or an enantiotropic system [3,8] could not be employed. At first glance, the fact that **1m** → **1o** phase change is endothermic suggested that the **1m/1o** system is enantiotropic with **1o** as the high-temperature polymorph, while **1m** would be thermodynamically stable phase at low temperatures [12,44]. However, distinguishing thermodynamic relation between the polymorphs is not always straightforward. In the cases where the solid–solid phase transition is of complicated nature, DSC traces can depend on many factors and the identification of the relation became difficult to determine [45]. To undoubtedly determine which polymorph is thermodynamically stable at room temperature, competitive slurry experiment in n-propanol/diethylether was performed. PXRD of the sample collected after 5 h of stirring confirmed that, from **1m/1o** mixture, **1m** transforms completely to **1o**. Hence, **1o** is thermodynamically stable phase between room temperature and melting point and the system is thus monotropic. Additionally, kinetic experiments, like addition of antisolvent (diethyl ether) and crystallization from the melt confirmed that **1m** is kinetically favored polymorph [25].

## 8. Conclusions

Pseudo-peptide **1** crystallizes in two polymorphic forms (**1m** and **1o**), concomitantly or as a pure phase depending on the solvent of crystallization. In both polymorphs, molecule **1** retains the same molecular conformation. The polymorphism of **1m** and **1o** is characterized by different stacking of identical two-dimensional layers in respective non-centrosymmetric space groups. In the lower UV region the crystalline polymorphs **1m** and **1o** show slight absorbance differences. The work presented here clearly defined thermodynamic relation between two forms in this monotropic polymorph system. **1m** is kinetically stable form and it transfers to the thermodynamically stable **1o** by heating or by application of various solvent-free methods at room temperature. These methodologies can be used for purification of the concomitant mixture and controllable synthesis of target phase. Since both polymorphs crystallize in non-centrosymmetric groups, polar  $P2_1$  and nonpolar  $P2_12_1$ , in our future work we will aim to grow crystals of suitable size for study of their non-linear optical properties.

## Acknowledgements

These materials are based on work financed by the Unity Through Knowledge Fund (Grant UKF-36/08), the Croatian Science Foundation (Grant HrZZ-02.04/23) and the Ministry of Science, Education and Sports of Croatia (Grant 098-0982904-2946). The authors thank Professor Dubravka Matković-Čalogović (Faculty of Science, University of Zagreb) for X-ray single crystal data collection and Dr. Ivan Halasz (Faculty of Science, University of Zagreb) for invaluable intellectual contributions to this work.

## Appendix A. Supplementary material

CCDC 870669 and 870670 contain the supplementary crystallographic data for **1m** and **1o**, respectively. These data can be obtained free of charge via <http://www.ccdc.cam.ac.uk/conts/retrieving.html>, or from the Cambridge Crystallographic Data Centre, 12 Union Road, Cambridge CB2 1EZ, UK; fax: (+44) 1223-336-033; or e-mail: [deposit@ccdc.cam.ac.uk](mailto:deposit@ccdc.cam.ac.uk). Supplementary data associated with this article can be found, in the online version, at <http://dx.doi.org/10.1016/j.molstruc.2012.07.026>.

## References

- [1] W.C. McCrone, in: D. Fox, M.M. Labes, A. Weissberger (Eds.), *Physics and Chemistry of the Organic Solid State*, vol. 2, Interscience Publishers, New York, 1965, p. 725.
- [2] G.R. Desiraju, *Science* 278 (1997) 404.
- [3] J. Bernstein, *Polymorphism in Molecular Crystals*, first ed., Oxford University Press Inc., New York, 2002, p. 29.
- [4] J. Bernstein, *Cryst. Growth Des.* 11 (2011) 632.
- [5] G.R. Desiraju, *Crystal Engineering: The Design of Organic Solids*, Elsevier, Amsterdam, 1989.
- [6] N. Blagden, R.J. Davey, *Cryst. Growth Des.* 3 (2003) 873.
- [7] J. Aaltonen, M. Alleso, S. Mirza, V. Koradia, K.C. Gordon, J. Rantanen, *Eur. J. Pharm. Biopharm.* 71 (2009) 23.
- [8] H.G. Brittain, *Polymorphism in Pharmaceutical Solids*, second ed., Informa Healthcare USA, Inc., New York, 2009.
- [9] P.N. Prasad, D.J. William, *Introduction to Nonlinear Optical Effects in Molecules and Polymers*, J. Wiley & Sons, New York, 1991.
- [10] T. Watanabe, H. Yamamoto, T. Hosomi, S. Miyata, in: J. Messier, F. Kajzar, P. Prasad (Eds.), *Organic Molecules for Nonlinear Optics and Photonics*, Kluwer Academic Publishers, Dordrecht, 1991, p. 151.
- [11] K-S. Huang, D. Britton, M.C. Etter, S.R. Byrn, *J. Mater. Chem.* 6 (1996) 123.
- [12] J. Bernstein, R.J. Davey, J.-O. Henck, *Angew. Chem. Int. Ed.* 38 (1999) 3440.
- [13] Z. Kokan, S.I. Kirin, *RSC Adv.* 2 (2012) 5729.
- [14] R.A. Storey, I. Ymén, *Solid State Characterization of Pharmaceuticals*, Blackwell Publishing, John Wiley & Sons, Chichester, UK, 2011.
- [15] M. Rubčić, D. Milić, G. Pavlović, M. Cindrić, *Cryst. Growth Des.* 11 (2011) 5227.
- [16] S.L. James, C.J. Adams, C. Bolm, D. Braga, P. Collier, T. Friščić, F. Grepioni, K.D.M. Harris, G. Hyett, W. Jones, A. Krebs, J. Mack, L. Maini, A.G. Orpen, I.P. Parkin, W.C. Shearouse, J.W. Steed, D.C. Waddell, *Chem. Soc. Rev.* 41 (2012) 413.
- [17] Oxford Diffraction, Oxford Diffraction Ltd., Xcalibur CCD system, CRYSTALLS Software system, Version 1.170.33.32, 2009.
- [18] A. Altomare, M.C. Burla, M. Camalli, G.L. Cascarano, C. Giacovazzo, A. Guagliardi, A.G.G. Moliterni, G. Polidori, R. Spagna, *J. Appl. Crystallogr.* 32 (1999) 115.
- [19] G.M. Sheldrick, *Acta Crystallogr., Sect. A: Found. Crystallogr.* 64 (2008) 112.
- [20] L.J. Farrugia, *J. Appl. Crystallogr.* 32 (1999) 837.
- [21] A.L. Spek, PLATON, Utrecht University, Utrecht, The Netherlands, A Multipurpose Crystallographic Tool, 2005.
- [22] L.J. Farrugia, *J. Appl. Crystallogr.* 30 (1997) 565.
- [23] C.F. Macrae, P.R. Edgington, P. McCabe, E. Pidcock, G.P. Shields, R. Taylor, M. Towler, J. van de Streek, *J. Appl. Crystallogr.* 39 (2006) 453.
- [24] Topas, version 4.1. Bruker-AXS, Karlsruhe, Germany, Single-crystal diffraction experiments for both polymorphs were conducted at 120 K and their calculated powder diffractograms differ from experimental diffractograms, measured by PXRD at room temperature. To obtain comparable data, both calculated spectra were refined by Pawley method in Topas.
- [25] G.P. Stahly, *Cryst. Growth Des.* 7 (2007) 1007.
- [26] IUPAC-IUB Commission on Biochemical Nomenclature, *J. Mol. Biol.* 52 (1970) 1.
- [27] J.J. McKinnon, M.A. Spackman, A.S. Mitchell, *Acta Crystallogr., Sect. B: Struct. Sci.* 60 (2004) 627.
- [28] M.A. Spackman, D. Jayatilaka, *CrystEngComm* 11 (2009) 19.
- [29] F.H. Allen, *Acta Crystallogr., Sect. B: Struct. Sci.* 58 (2002) 380.
- [30] T.C. van Soest, A.F. Peerdeman, *Acta Crystallogr., Sect. B: Struct. Sci.* 26 (1970) 1947.
- [31] T.N. Drebushchak, N.V. Chukanov, E.V. Boldyreva, *Acta Crystallogr., Sect. C: Cryst. Struct. Commun.* 63 (2007) o355.
- [32] T.N. Drebushchak, Y.A. Chesalov, E.V. Boldyreva, *Acta Crystallogr., Sect. B: Struct. Sci.* 65 (2009) 770.
- [33] E. Sugiono, M. Bolte, *Acta Crystallogr., Sect. C: Cryst. Struct. Commun.* 64 (2008) o84.
- [34] M. Rubčić, K. Užarević, I. Halasz, N. Bregović, M. Mališ, I. Đilović, Z. Kokan, R.S. Stein, R.E. Dinnebier, V. Tomišić, *Chem. Eur. J.* 18 (2012) 5620.
- [35] P.S. Halasyamani, K.R. Poeppelmeier, *Chem. Mater.* 10 (1998) 2753.
- [36] K.T. Holman, A.M. Pivovarov, M.D. Ward, *Science* 294 (2001) 1907.
- [37] D. Braga, D. D'Addario, S.L. Gialfreda, L. Maini, M. Polito, F. Grepioni, *Top. Curr. Chem.* 254 (2005) 71.
- [38] T. Friščić, *J. Mater. Chem.* 20 (2010) 7599.
- [39] W.J. Belcher, C.A. Longstaff, M.R. Neckenig, J.W. Steed, *Chem. Commun.* (2002) 1602.
- [40] D. Cinčić, I. Brekalo, B. Kaitner, *Cryst. Growth Des.* 12 (2012) 44.
- [41] K. Užarević, M. Rubčić, I. Đilović, Z. Kokan, D. Matković-Čalogović, M. Cindrić, *Cryst. Growth Des.* 9 (2009) 5327.
- [42] M. Descamps, J.F. Willart, E. Dudognon, V. Caron, *J. Pharm. Sci.* 96 (2007) 1398.
- [43] T. Friščić, *Chem. Soc. Rev.* 41 (2012) 3493.
- [44] F.H. Herbstein, *Acta Crystallogr., Sect. B: Struct. Sci.* 62 (2006) 341.
- [45] D. Khamar, I.J. Bradshaw, G.A. Hutcheon, L. Seton, *Cryst. Growth Des.* 12 (2012) 109.